Mitochondrion 89 (2026) 102149

Contents lists available at ScienceDirect

Mitochondrion

journal homepage: www.elsevier.com/locate/mito

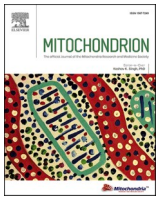

Original Research Article

Impact of compound heterozygous *SDHA* variants on mitochondrial function in pediatric with neurological disease

Rocío Garrido-Moraga [a,b], Pablo Serrano-Lorenzo [a,b,1], María J. Esteban-Amo [c,d], Marcello Bellusci [a,b,e], Miguel Á. de la Fuente [c,d], Joaquín Arenas [a,b], Adrián González-Quintana [a,b], Cristina Ugalde [a,f], María Simarro [c,d,*], Miguel A. Martín [a,b,g]

[a] *Spanish Network for Biomedical Research in Rare Diseases (CIBERER), Instituto de Salud Carlos III, 28029 Madrid, Spain*
[b] *Mitochondrial and Neuromuscular Research Group, '12 de Octubre' Hospital Research Institute (imas12), 28041 Madrid, Spain*
[c] *Department of Cell Biology, Genetics, Histology and Pharmacology, Faculty of Medicine, University of Valladolid 47005 Valladolid, Spain*
[d] *Unit of Excellence Institute of Biomedicine and Molecular Genetics (IBGM), University of Valladolid and Spanish National Research Council (CSIC), 47003 Valladolid, Spain*
[e] *Reference Center for Inherited Metabolic Disorders, MetabERN Center "12 de Octubre" University Hospital, 28041 Madrid, Spain*
[f] *Margarita Salas Center for Biological Research (CIB-CSIC), 28040 Madrid, Spain*
[g] *Genetics Service, Hospital Universitario "12 de Octubre", 28041 Madrid, Spain*

ARTICLE INFO

Keywords:
SDHA gene
Compound heterozygous mutations
Mitochondrial dysfunction
Neurological disorders

ABSTRACT

This study examines two rare compound heterozygous missense variants in the *SDHA* gene, c.1535G > A (p.R512Q) and c.1753C > T (p.R585W), identified in a pediatric patient presenting with neurological manifestations, including epilepsy, developmental delay, and optic atrophy. The *SDHA* gene encodes a key component of succinate dehydrogenase (SDH), an essential enzyme complex at the intersection of two fundamental metabolic pathways: the Krebs cycle, and the mitochondrial respiratory chain (MRC).

Patient-derived fibroblasts were used to evaluate the impact of the mutations on SDH activity and MRC assembly and function. The analysis revealed significant decreases in SDH activity and subunit levels, as well as impaired assembly. Additionally, complex I (CI) activity and CI-containing supercomplexes formation were also impaired, indicating more widespread mitochondrial dysfunction. Unexpectedly, basal and maximal respiration rates remained unchanged, though spare respiratory capacity was significantly reduced. These findings demonstrate the deleterious effects of the c.1535G > A and c.1753C > T variants, which had previously been associated with primary mitochondrial disorder (PMD) and tumors but had not been functionally validated until now.

1. Introduction

Mitochondrial diseases are a genetically heterogeneous group of pathologies caused by defects in genes that encode proteins essential for mitochondrial oxidative phosphorylation (OXPHOS), which is the central process of cellular energy generation (Ng and Turnbull, 2016). Despite being one of the most common groups of genetic diseases, the low incidence of each individual disease poses a significant challenge to developing specific treatments (Darin et al., 2001). Addressing these rare diseases requires conducting enzymatic, respirometric, and structural studies of genetic variants suspected to be pathogenic to better understand their mechanisms and develop specific treatments.

The OXPHOS system is essential for ATP production and includes the mitochondrial respiratory chain (MRC), which is composed of four multiprotein complexes, and ATP synthase (Pfanner et al., 2019). All of the complexes are encoded partly by mitochondrial DNA (mtDNA) and

* Corresponding author at: Department of Cell Biology, Genetics, Histology and Pharmacology, Faculty of Medicine, University of Valladolid, 47005 Valladolid, Spain.

E-mail addresses: rociogarridorgm@gmail.com (R. Garrido-Moraga), pabloserralor@gmail.com (P. Serrano-Lorenzo), mariajesus.esteban@uva.es (M.J. Esteban-Amo), marcello.bellusci@salud.madrid.org (M. Bellusci), miguelafuente@gmail.com (M.Á. de la Fuente), joaquin.arenas@salud.madrid.org (J. Arenas), agonzalez.imas12@h12o.es (A. González-Quintana), cristina.ugalde@cib.csic.es (C. Ugalde), maria.simarro.grande@uva.es (M. Simarro), mamcasanueva.imas12@h12o.es (M.A. Martín).

[1] Current address: Genetics Department, Hospital La Paz, 28046 Madrid, Spain.

https://doi.org/10.1016/j.mito.2026.102149
Received 21 November 2025; Received in revised form 22 February 2026; Accepted 10 March 2026
Available online 13 March 2026

partly by nuclear DNA (nDNA), except for complex II (CII), which is entirely encoded by nDNA (Anderson et al., 1981). CII, also known as succinate dehydrogenase (SDH/CII), has another distinguishing feature: it is the only OXPHOS complex involved in the Krebs cycle, where it converts succinate to fumarate. SDH/CII is the smallest complex in the MRC, consisting of four subunits: SDHA, SDHB, SDHC, and SDHD. SDHA contains an active site with FAD, which catalyzes the oxidation of succinate to fumarate. SDHB carries iron-sulfur clusters that transfer electrons to the ubiquinone pool, while SDHC and SDHD anchor the complex to the inner mitochondrial membrane and facilitate the reduction of ubiquinone. Four assembly factors have been reported to play a role in the maturation of holo-SDH/CII: SDH assembly factor 1 (SDHAF1), SDHAF2, and the chaperone-like SDHAF3 and SDHAF4 (Bezawork-Geleta et al., 2017; Iverson et al., 2023; Rutter et al., 2010).

Mutations in the *SDHA, SDHB, SDHC*, and *SDHD* genes, as well as the *SDHAF1* and *SDHAF2* genes, disrupt mitochondrial function. This can lead to congenital mitochondrial diseases or an increased risk of tumor development (Bezawork-Geleta et al., 2017; Rutter et al., 2010). Congenital SDH/CII deficiencies are rare. They are mostly caused by biallelic pathogenic variants in the *SDHA* gene and are frequently associated with severe neurological disorders, such as Leigh syndrome (Koopman et al., 2012). In contrast, monoallelic *SDHx* pathogenic variants can predispose individuals to neuroendocrine tumors, including pheochromocytomas (PCC) and paragangliomas (PGL), with *SDHB* and *SDHD* mutations being the most frequent. These tumors exhibit loss of heterozygosity, indicating the role of *SDHx* genes as tumor suppressors. *SDHx* mutations have also been associated with gastrointestinal stromal tumors (GIST), as well as renal and pituitary tumors (Dwight et al., 2013; Gault et al., 2018).

In this study, we identified two rare compound heterozygous variants in the *SDHA* gene, c.1535G > A and c.1753C > T, in a 14-year-old patient presenting with neurological manifestations. These variants were recently reported in a 4-year-old patient with primary mitochondrial disease (PMD) within the framework of a study examining cognitive functioning and mental health in children with PMD, although no data were provided regarding their pathogenic effects (van de Loo et al., 2022). Likewise, the c.1753C > T (p.R585W) variant has been previously documented in a few patients with PCC, PGL, and GIST tumors (Boikos et al., 2016; Korpershoek et al., 2011). Here, we describe experimental validation of these *SDHA* variants for the first time by examining their impact on SDH/CII activity and the function and assembly of the MRC complexes in patient-derived skin fibroblasts.

2. Patient and methods

2.1. Case report

The subject of this study is a 14-year-old male born to a healthy, non-consanguineous couple. He presented with a severe neurodevelopmental disorder characterized by global psychomotor delay, profound intellectual disability, and autistic features. He also exhibited symptomatic epilepsy with brief staring seizures and EEG epileptiform discharges induced by eyelid closure. Neurological examination revealed an equinus gait. Brain MRI demonstrated T2/FLAIR hyperintensities involving the brainstem and spinal cord, along with diffuse white matter abnormalities. Ophthalmological evaluation showed bilateral optic nerve atrophy. No further longitudinal neurodevelopmental assessments were available. Laboratory findings included persistent neutropenia, thrombocytopenia, and elevated postprandial lactate levels. All these findings were strongly suggestive of a mitochondrial disorder and prompted further genetic and functional studies, which are detailed in this report. Given the eventual identification of a variant in an SDH-related gene, personal and family history were specifically reviewed, and no history of SDH-associated tumors was reported. The study was approved by the Ethics Committee of the 'Hospital Universitario 12 de Octubre' (Madrid, Spain) (protocol code: 22/144, date of approval: 26/04/2022) and was performed in accordance with the Declaration of Helsinki for Human Research. Written informed consent to participate in this study was obtained from the parents of the patient and healthy donors prior to their participation in this study.

2.2. Sequencing and data analysis

Genomic DNA (gDNA) from the patient and healthy donors was extracted from whole blood using the NZY Tissue gDNA Isolation Kit (NZYTech). Since a mitochondrial disorder was highly suspected, targeted sequencing using a customized NSG OXPHOS panel previously developed in our laboratory (González-Quintana et al., 2020), was selected as a first-tier genomic approach. This panel ~~which~~ includes 133 genes (Table S1) encoding structural subunits and assembly factors of the OXPHOS system. This phenotype-driven strategy was prioritized over more standard first-line genomic tests for neurodevelopmental disorders, such as array CGH or whole exome sequencing. Annotation and prioritization of variants was done through the integration of in-house scripts with Annovar (Wang et al., 2010). Variant prioritization was based assuming an autosomal recessive inheritance following the next steps: (1) status of the variants in the ClinVar database; (2) minor allele frequency (MAF) < 0.01 in population databases such as the Genome Aggregation Database (gnomAD, https://gnomad.broadinstitute.org) and 1000 genomes project database (https://browser.1000genomes.org); (3) pathogenicity predictions from SIFT (http://sift-dna.org), PolyPhen-2 (http://genetics.bwh.harvard.edu/pph2), and CADD Phred (https://cadd.gs.washington.edu), and splicing predictors such as dbNSFP (https://sites.google.com/site/jpopgen/dbNSFP), dPSI (difference in percentage spliced in) and Human Splicing Finder (https://www.umd.be/HSF3/); and (4) assessment of phylogenetic conservation using Genomic Evolutionary Rate Profiling ++ (GERP++) (https://bio.tools/gerp) and the Phylogenetic Analysis with Space/Time models (PHAST) programs: phastCons and phyloP (http://compgen.cshl.edu/phastweb/). Additionally, variants pathogenicity was evaluated using the American College of Medical Genetics and Genomics (ACMG) guidelines (Richards et al., 2015). Sanger sequencing was performed on the proband and his parents to confirm the presence and segregation of the candidate variants in the *SDHA* gene (Table S2).

2.3. Protein modeling and conservation analysis

The SDHA variants p.(R512Q) and p.(R585W) were modeled using the SWISS-MODEL server (Waterhouse et al., 2018), with the Cryo-EM structure of the human respiratory complex II (PDB ID: 8GS8) as template (Du et al., 2023). The overlay of the wild-type and mutant residues was generated. Structural visualization and figure preparation were carried out using ChimeraX (v1.9) (Pettersen et al., 2021). The SDHA variants p.(R512Q) and p.(R585W), the human wild-type sequence, and orthologues from five species (*Mus musculus*, *Gallus gallus*, *Danio rerio*, *Xenopus laevis*, and *Drosophila melanogaster*) were retrieved from the NCBI Protein Database and aligned using Clustal Omega software (Sievers et al., 2011).

2.4. Skin fibroblasts cultures

Cultured fibroblasts were derived from skin biopsies. Fibroblasts from the patient and healthy donors were cultured in Dulbecco Modified Eagle Medium (DMEM) (Lonza) with 4.5 g/L glucose supplemented with L-glutamine, 10% fetal bovine serum (Biowest) and 1% penicillin/streptomycin (Gibco, ThermoFisher Scientific). Cultures were maintained at 37 °C in a humidified 5% CO2 atmosphere.

2.5. MRC complexes activities

Respiratory chain complexes activities in fibroblasts and skeletal

muscle were measured spectrophotometrically according to the method of Bujan et al. (Bujan et al., 2022). Two 175 cm^2 flasks of confluent cells were collected by centrifugation at 800 x g for 5 min. Pellets were resuspended in 300 µL homogenization buffer (mannitol buffer). The mannitol buffer pH 7.2 consisted of 225 mM D-mannitol, 75 mM sucrose, 10 mM Tris-HCl and 0.1 mM EDTA. The cell suspension was sonicated twice for 5 s at 200 W in an ice bath. Cell homogenates were maintained in the ice bath prior to the spectrophotometric enzyme assays.

2.6. Mitochondrial respiration assays

Oxygen consumption rate (OCR) in fibroblasts was assessed in the extracellular analyzer XFp (Seahorse Agilent Technologies). Mitochondrial respiration assays were performed following the described protocol (Morán et al., 2010) with minor modifications in reagents concentrations: 2.6 µM oligomycin (#75351, Sigma-Aldrich), 1.0 µM carbonyl cyanide 4-(trifluoromethoxy)-phenyl-hydrazone (FCCP) (C2920, Sigma-Aldrich) and 1.0 µM rotenone/antimycin A (R8875 and A8674, respectively, both from Sigma-Aldrich). 40,000 cells/well were seeded for approximately 24 h on XFp plates prior to performing the test. Data was obtained using Agilent Seahorse Wave 2.6.3.5 software (Seahorse Agilent Technologies).

2.7. Preparation of fibroblasts mitochondria

Mitochondrial isolation was performed as described previously (Fernández-Vizarra et al., 2010). Cells were trypsinized, pelleted (600 × g, 5 min), and washed twice with ice-cold PBS. Pellets on ice were swollen by adding 1 vol of hypotonic homogenization buffer (3.5 mM Tris-HCl, pH 7.8; 2.5 mM NaCl; 0.5 mM $MgCl_2$) and homogenized with 10 S in a manual glass–Teflon homogeneizer with smooth pestle (Thomas). Isotonicity was restored by adding 1/10 vol of hypertonic buffer (0.35 M Tris-HCl, pH 7.8; 0.25 M NaCl; 50 mM $MgCl_2$). The homogenate was cleared of nuclei and debris (1,200 × g, 3 min, 4 °C); the supernatant was collected and the spin repeated once. Mitochondria in the resultant supernatant were pelleted (15,000 × g, 2 min, 4 °C), washed three times in STE (0.32 M sucrose; 1 mM EDTA; 10 mM Tris-HCl, pH 7.4) and resuspended in STE to 10–15 mg/mL. Protein was quantified with the Pierce MicroBCA assay (Thermo Fisher Scientific).

2.8. Protein gel electrophoresis

Mitochondrial protein extracts were separated by either sodium dodecyl-sulfate polyacrylamide gel electrophoresis (SDS-PAGE) or blue native polyacrylamide gel electrophoresis (BN-PAGE). For SDS–PAGE, mitochondrial pellets corresponding to 30–40 µg of protein were resuspended in 4x Laemmli sample buffer (Bio-Rad) and separated on 4–20% Tris–Glycine gels (Invitrogen Novex). For BN-PAGE, mitochondrial protein extracts were prepared as previously described (Timón-Gómez et al., 2020). Briefly, mitochondrial pellets were resuspended in a buffer containing 1.5 M aminocaproic acid and 50 mM Bis-Tris (pH 7.0). Samples were solubilized using digitonin at a detergent-to-protein ratio of 4:1 and incubated on ice for 15 min. After centrifugation at 20,000 x g for 30 min at 4 °C, the supernatant was mixed with 10x native sample buffer (750 mM aminocaproic acid, 50 mM Bis-Tris, 0.5 mM EDTA, 5% Coomassie Brilliant Blue G-250) prior to loading. Invitrogen NativePAGE 3–12% Bis-Tris mini protein gels (Thermo Fisher Scientific) were loaded with 30–40 µg of mitochondrial protein. Following electrophoresis, proteins were transferred to polyvinylidene fluoride (PVDF) membranes.

2.9. Western blotting

After electroblotting the proteins onto PVDF membranes, they were detected by incubating the membranes with the following antibodies: anti-ATP5B (ab128743, Abcam, at 1:10,000 dilution), anti-NDUFA9 (ab14713, Abcam, at 1,000 dilution), total OXPHOS human WB antibody cocktail (ab110411, Abcam, at 1:250 dilution), anti-SDHA (ab14715, Abcam, at 10,000 dilution), anti-SDHB (ab14714, Abcam, at 1:1,000 dilution), anti-SDHC (ab155999, Abcam, at 1:1,000 dilution), anti-SDHD (ab189945, Abcam, at 1:1,000 dilution), anti-UQCR2 (ab14745, Abcam, at 1,2000 dilution), anti-COX4 (ab62164, Abcam at 1:4,000 dilution), and anti-COX5A (ab110262, Abcam, at 1:1,000 dilution). Immunoreactive bands were detected with ECL Prime Western Blotting Detection Reagent (GE Healthcare, Amersham, UK) in a ChemiDoc™ MP Imaging System (Bio-Rad, Hercules, CA, USA). The optical densities of the immunoreactive bands were measured using NIH ImageJ software v1.8 (Wayne Rasband, NIH, Bethesda, MD, USA). Densitometric analyses of SDS-PAGE and BN-PAGE immunoblots were normalized to ATP5B as a mitochondrial loading control.

2.10. Statistical analysis

Statistical analyses were performed using GraphPad Prism software. Mann-Whitney *U* test (two-tailed) were used when comparing two groups. Test values of $p < 0.05$ were considered statistically significant. In the figures, each point represents a biological replicate and, if no other indication is made, data are expressed as the mean ± SD.

3. Results

3.1. Genetic findings

To investigate the genetic basis of the patient's phenotype, we performed a customized NGS panel targeting 133 genes encoding OXPHOS structural subunits and assembly factors (Table S1). The analysis identified two missense variants in the *SDHA* gene (Fig. 1A), the c.1535G > A (p.R512Q) in exon 11 and c.1753C > T (p.R585W) in exon 13 of transcript NM_004168.4. No additional potentially pathogenic variants related to the patient's phenotype were detected.

These variants were previously documented in a 4-year-old pediatric patient with primary mitochondrial disease (PMD) in a study examining cognitive function and mental health in children with PMD, although their pathogenicity was not evaluated (van de Loo et al., 2022). The c.1753C > T variant has been also reported in association with PCC, PGL, and GIST autosomal dominant tumors (Boikos et al., 2016; Korpershoek et al., 2011). Experimental validation of the pathogenicity of both variants has not been previously explored.

Both variants are rare, with an allele frequency below 0.01% in population databases. Furthermore, pathogenicity prediction tools including SIFT, PolyPhen-2, and CADD Phred consistently indicated that both variants are likely deleterious (Fig. 1A). The affected amino acids, depicted in the 3D structure of the SDHA protein (Fig. 1C), are highly conserved across species, further supporting their potential pathogenicity. Both variants are registered in ClinVar as variants of uncertain significance (VUS) with six submitters for c.1535G > A and eight for c.1535G > A.

Family segregation analysis by Sanger sequencing confirmed the presence of the two variants in the proband and showed that the mother carried the c.1535G > A and the father the c.1753C > T, each in heterozygous state (Fig. 1B), indicating compound heterozygosity in the proband. According to ACMG criteria, the c.1535G > A variant was classified as VUS including as supporting the PP1 co-segregation criterion (PM2, PP3 and PP1), while the c.1753C > T was classified as pathogenic based on multiple ACMG criteria (PS4, PS1, PM5, PM2, PP3, PM1 and PP1) and is supported by its association with germline autosomal dominant rare tumors.

3.2. Analysis of the activity of the MRC complexes

To evaluate the pathogenicity of the SDHA variants, the activities of

A

SDHA gene variants	zygosity	gnomAD	SIFT	PolyPhen2	CADD phred	GERP++	PhyloP
Exon 11: c.1535G>A; p.Arg512Gln	Heterozygous	0,00002	D (Deleterious)	D (Deleterious)	20,5	4,95 (Highly preserved)	9,24 (Highly preserved)
Exon 13: c.1753C>T; p.Arg585Trp	Heterozygous	0,000023	D (Deleterious)	D (Deleterious)	15,78	3,79 (Preserved)	5,375 (Preserved)

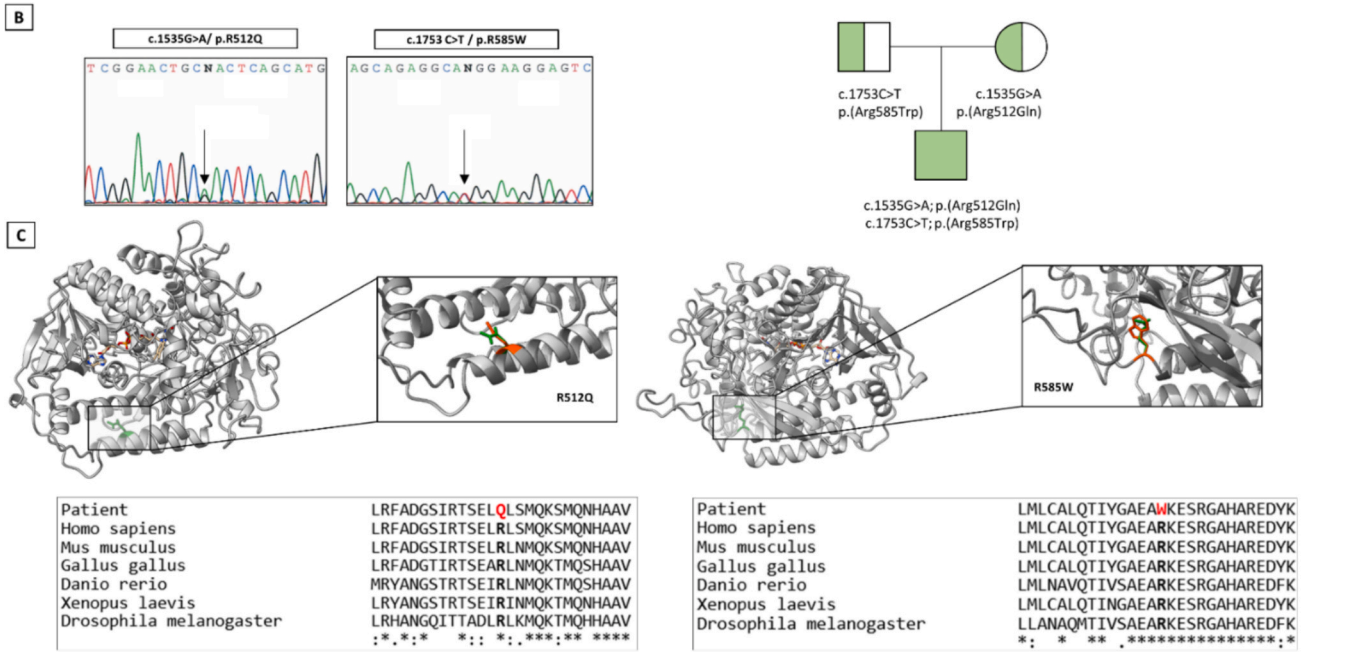

Fig. 1. Identification of SDHA variants in the patient with potential pathogenic effect. (A) Two prioritized variants in SDHA and their predictor scores identified through the OXPHOS panel analysis. CADD ≥ 10 indicates that the variant ranks among the top 10% most deleterious in the human genome, whereas CADD ≥ 20 corresponds to the top 1% most deleterious variants. D stands for damaging. (B) Sanger sequencing and pedigree of the family showing the segregation of both variants. (C, top) Structural analysis of p.(R512Q) and p.(R585W). Insets highlight the wild-type and mutant residues in green and red, respectively. Bottom panel, Evolutionary conservation of the SDHA region containing residues R512Q and R585W, highlighted in red. (For interpretation of the references to colour in this figure legend, the reader is referred to the web version of this article.)

the MRC complexes were measured spectrophotometrically in mitochondria-enriched preparations obtained from skin cultured fibroblasts and skeletal muscle of the patient. Complexes activities were normalized to the mitochondrial matrix enzyme, citrate synthase (Table 1). Compared with controls, patient fibroblasts showed a significant reduction in CII activity. No significant differences in CIII or CIV activities were detected between patient and control fibroblasts. Interestingly, CI activity was also decreased in patient fibroblasts, whereas it remained normal in skeletal muscle.

Next, we evaluated the impact of the deficient CII and CI activities on the respiratory capacity of the patient fibroblasts. Surprisingly, basal OCR, maximal OCR, and ATP production, were normal. However, the spare respiratory capacity was significantly reduced in the patient fibroblasts (Fig. 2).

Table 1
Mitochondrial respiratory chain enzyme activities in the patient skeletal muscle and fibroblasts. (1, 3) Complexes activities expressed as nmol min^{-1} mg^{-1} relative to citrate synthase (CS) activity. (1) Skeletal muscle enzymatic activities are reported according to an established clinical reference range (2.5th–97.5th percentile; n = 95), which represents standardized diagnostic laboratory practice. (2) % of complex activity relative to the 2.5th percentile of controls. (3) Fibroblast measurements were performed in parallel with three independent control cell lines (n = 3). Control values are expressed as mean ± SD. (4) % of complex activity relative to the mean control values. (5) CS activity expressed as nmol min^{-1} mg^{-1} protein.

	Skeletal Muscle		Fibroblasts	
	Patient (Controls)[1]	**%[2]**	**Patient (Controls)[3]**	**%[4]**
CI NADH-Decylubiquinone oxidoreductase	13.1 (11.3–24.7)	116%	9.9 (15.4 ± 3.3)	64.3%
CII Succinate dehydrogenase	2.7 (5.8–19.9)	45.5%	18.6 (64.9 ± 18.1)	28.6%
CIII Decylubiquinol-cytochrome c oxidoreductase	58.5 (31–127)	188%	71.9 (59.8 ± 5.9)	120.2%
CIV Cytochrome c oxidase	38.1 (20–79.2)	190.5%	96.5 (96.8 ± 2 2.5)	99.6%
CS Citrate synthase[5]	303.4 (102–257)	–	50.8 (67.9 ± 17.1)	–

3.3. *Analysis of the assembly of the MRC complexes*

Prior to investigating the assembly of MRC complexes and supercomplexes (SCs) in patient fibroblasts, we analyzed the levels of various OXPHOS proteins isolated by SDS-PAGE. The mutations caused a decrease in SDHA expression, likely due to protein instability. Since SDHA is the final subunit to assemble into complex II (CII) and is the most stable in its free form (Cao et al., 2023), the reduction of the remaining subunits, with SDHC being nearly undetectable in patient fibroblast lysates compared to control fibroblasts, was not unexpected. Additionally, a decrease was observed in the NDUFA9 subunit, which is part of the Q module of CI, while the levels of CORE2 (CIII), COX4 (CIV), and ATP5B (CV) remained normal (Fig. 3).

Finally, we assessed the distribution of free MRC complexes and SCs using 1D BN-PAGE followed by Western blot analysis (Fig. 4). As expected, mutant cells showed a significant decrease in CII assembly, as evidenced by SDHA and SDHC antibodies. Additionally, a significant

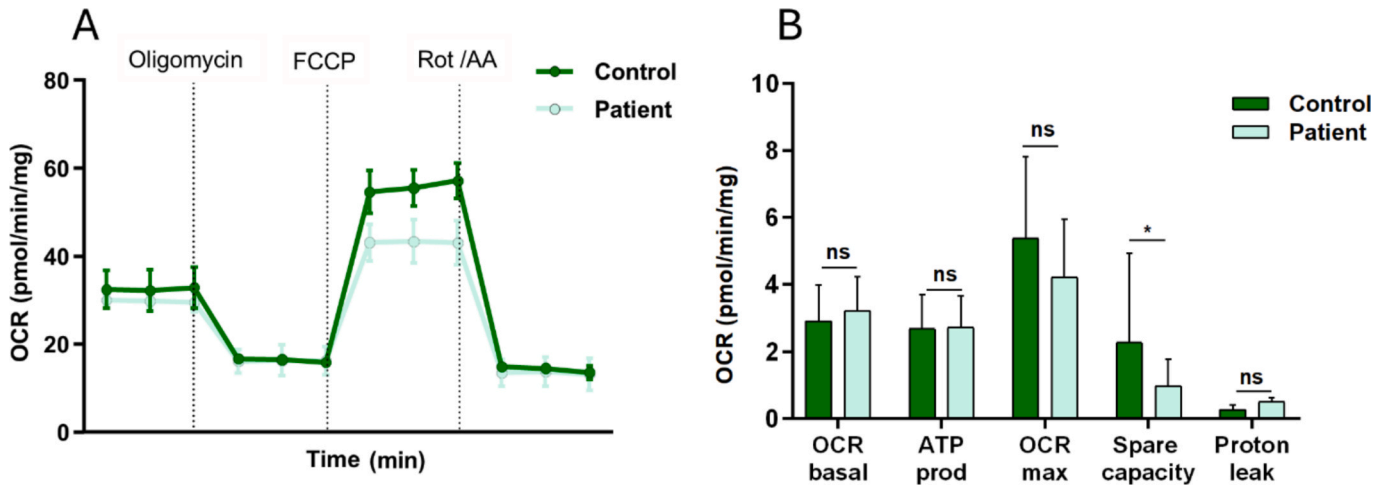

Fig. 2. Oxygen consumption rates and respiration parameters in the patient fibroblasts. (A) A representative experiment showing OCR in control and patient fibroblasts before and after the sequential addition of oligomycin (2.6 μM), FCCP (1 μM), and a combination of rotenone (Rot) and antimycin A (AA) (1 μM). (B) Mitochondrial parameters (basal respiration, proton leak, maximal respiration, spare respiratory capacity, ATP production) are shown. Ns, not significant; *, $P < 0.05$, Mann-Whitney *U* test. Data are shown as the mean ± SD.

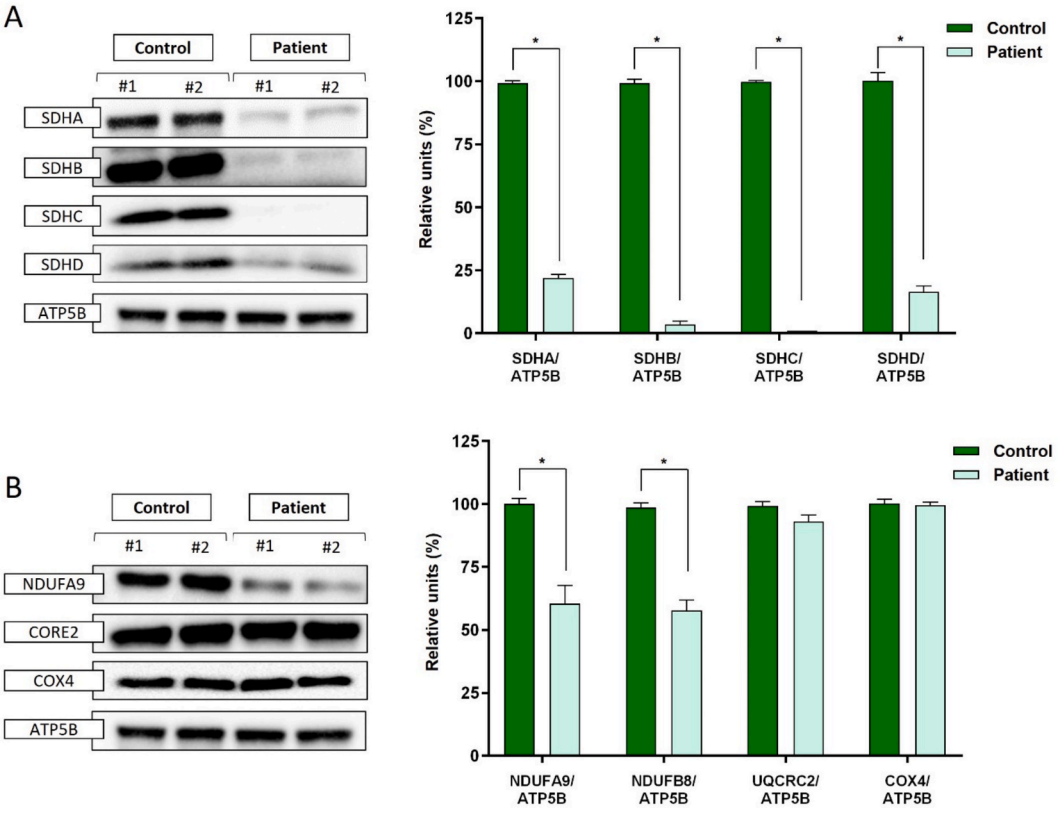

Fig. 3. Expression of MRC complexes subunits. (A) Mitochondrial proteins extracted from control and patient fibroblasts were analyzed by SDS-PAGE, followed by immunodetection using antibodies against CI (NDUFA9), CII subunits (SDHA-D), and CIII (Core 2). Equal amounts of protein were loaded in all lanes. ATP5B was used as a loading control. Samples #1 and #2 refer to different replicates of the same experiment. (B) Densitometric analyses of SDS-PAGE and BN-PAGE immunoblots were normalized to ATP5B as a mitochondrial loading control. Data represent mean densities ± SD from at least three independent experiments.

decrease in CI-containing SCs, including the respirasome (CI + $CIII_2$+CIV_n), was detected with a NDUFA9 antibody. In contrast, CIII levels in patient cells were comparable to controls, as assessed by immunodetection with a CORE2 antibody, both in its dimeric form ($CIII_2$) and in SCs containing CIV and CI. A slight reduction in SC I + $CIII_2$ abundance was observed; however, this decrease did not reach statistical significance. CIV, detected using a COX5A antibody, was present at levels comparable to controls in its monomeric and dimeric forms, as well as within higher-order assemblies with CIII and CI. The monomeric CIV species showed a very mild reduction that was also not statistically significant. Thus, a decrease in CI-containing SCs was detected exclusively with the CI antibody (NDUFA9). Because CI is present as a single copy and may represent a limiting structural component, its reduction can selectively attenuate the CI-derived

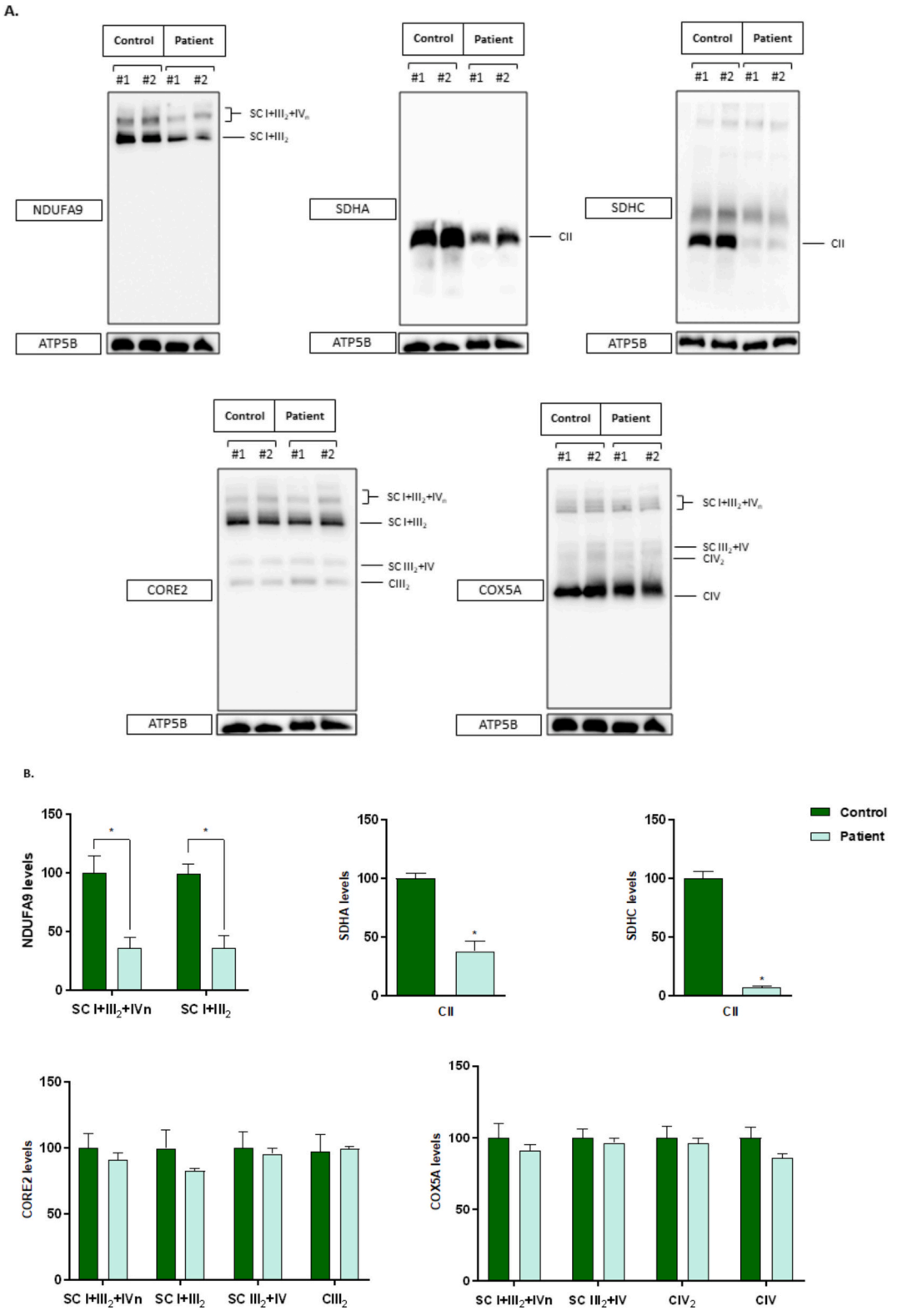

Fig. 4. Analysis of mitochondrial complexes and SCs. (A) 1D-BNE showing OXPHOS complexes I to IV (CI-CIV) and SCs. Western blot analysis was performed using antibodies against CI (NDUFA9), CII (SDHA and SDHC), CIII (Core 2), and CIV (COX5A). Equal amounts of protein were loaded in all lanes. Loading control, CV subunit ATP5B. Samples #1 and #2 refer to different replicates of the same experiment. (B) Densitometric analyses of SDS-PAGE and BN-PAGE immunoblots were normalized to ATP5B as a mitochondrial loading control. Data represent mean densities ± SD from at least three independent experiments.

respirasome signal without proportionally affecting the $CIII_2$- or CIV-derived signal.

3.4. *Reclassification of pathogenicity of SDHA variant*

The previous findings indicating evidence of an impact on mitochondrial function resulted from the presence of the two *SDHA*

compound heterozygous variants in SDHA, enables to apply the PS3 criterion (functional studies) of ACMG guidelines to reclassify the c.1535G > A (p.R512Q) variant from VUS to likely pathogenic, and experimentally reinforce the classification as pathogenic of the c.1753C > T (p.R585W) variant.

4. Discussion

We present a 14-year-old male presenting with neurological phenotype characterized by epilepsy, psychomotor delay, intellectual disability, and partial optic atrophy. Using a customized NGS panel targeting genes encoding components of the OXPHOS system, we identified compound heterozygous variants in *SDHA* – c.1535G > A (p.R512Q) and c.1753C > T (p.R585W), which encodes SDHA, the major catalytic subunit of SDH/CII.

The clinical phenotype associated with *SDHA* mutations shows wide variability. Autosomal reccesive biallelic *SDHA* mutations are most commonly associated with Leigh or Leigh like syndromes presenting in infancy or early childhood, cardiomyopathy, leukodystrophy, neuropathy and neuromuscular disease. In contrast, dominant inheritance has been reported in families presenting with late-onset optic atrophy, ocular movement disorders, cardiomyopathy, ataxia and cerebellar signs (H Sturrock et al., 2021). Our patient's clinical picture is consistent with the neurological spectrum reported in autosomal recessive *SDHA*-related PMD, although the later age of clinical manifestation and less prominent multisystem involvement compared to typical infantile Leigh phenotypes suggest a milder disease course (Alston et al., 2012; Fullerton et al., 2020; Renkema et al., 2015).

Notably, these same *SDHA* variants were recently documented in a 4-year-old male patient within a cohort study examining cognitive function and mental health in children with PMD (van de Loo et al., 2022), who presented at 6 months of age with clinical features overlapping with our patient, including low IQ, motor disability and epilepsy; however, he did not show any vision problems. The absence of functional assessment of these variants in that report left their pathogenic impact unclear in the context of autosomal recessive *SDHA*-related PMD. In the current study, we provide the first functional evidence demonstrating that these variants result in loss of function, establishing a direct molecular basis for the clinical phenotypes observed in both patients.

In the current study, the patient's fibroblasts showed a dramatic decrease in SDH/CII activity and assembly, as well as a reduction in the steady-state levels of all its subunits. A significant decrease in CI activity and CI-containing SCs, including the respirasome, was also observed. The decrease in CI activity has been previously described in various cellular models of SDH/CII deficiency (Bezawork-Geleta et al., 2018; Cardaci et al., 2015; Hart et al., 2023; Lorendeau et al., 2017) and has been proposed to serve as an adaptive mechanism (Hart et al., 2023; Lorendeau et al., 2017). Notably, one study shows that the loss of CI is beneficial for CII-deficient cells by increasing their production of aspartate, their proliferation rate, and their capacity for tumor growth (Hart et al., 2023). These findings support the concept that down-regulation of CI in the context of CII impairment is not merely a secondary defect but may represent a metabolic rewiring that allows cells to maintain biosynthetic capacity. In contrast, no reduction in CI activity was observed in skeletal muscle, which could be explained by the higher stability of SCs in this tissue as well as by the ability of muscle to preferentially rely on OXPHOS as its primary energy source (Greggio et al., 2017; Ikeda et al., 2013). Consistent with this tissue-specific effect, adrenally derived SDH/CII-deficient cells have also been reported to preserve CI activity despite marked cellular and mitochondrial morphological alterations (Al Khazal et al., 2024). One limitation of our study is that we were unable to assess the stability of SCs in the patient's skeletal muscle due to limited biopsy material. Collectively, these observations indicate that the biochemical impact of SDHA variants is likely tissue-dependent. Such variability may reflect differential metabolic plasticity across tissues, whereby energetically demanding organs such as skeletal muscle and adrenal medulla engage compensatory mechanisms that partially offset the downstream consequences of SDH/CII instability, in contrast to fibroblast cell culture models.

The impairments in CII and CI observed in the patient's fibroblasts were associated only with a significant reduction in spare respiratory capacity, but not with changes in other respiratory parameters. Although a decrease in maximal OCR was detected, it was not significant. This indicates that, under basal conditions, mitochondrial function is largely preserved and is still capable of supporting routine energetic demands. Taken together, these data suggest that the reduction in CI activity and assembly observed in the patient's fibroblasts, which represents the primary entry point for electrons into the MRC, was not sufficient to alter either basal or maximal respiration. Instead, the main functional consequence was a reduced ability to increase mitochondrial respiration under stress. The selective decrease in spare respiratory capacity is consistent with previous studies that highlight the role of SDH/CII in maintaining respiratory reserve across a range of cell types, including cardiac myocytes. (Chen et al., 2024; Dhingra and Kirshenbaum, 2015). Conceptually, preservation of basal respiration alongside a marked reduction in respiratory reserve suggests a state in which the system can sustain day-to-day ATP production but has a diminished capacity to respond to acute increases in energy demand or to mitochondrial stress. This bioenergetic profile suggests the presence of underlying metabolic adaptations, warranting future metabolomic analyses to more precisely delineate alterations in central carbon metabolism associated with SDH/CII deficiency.

Overall, our functional data supports the pathogenicity of the *SDHA* variants c.1535G > A (p.R512Q) and c.1753C > T (p.R585W) in the context of PMD. In particular, the evidence allowed to reclassify c.1535G > A from a VUS to likely pathogenic, and it broadens current understanding of how specific amino acid substitutions in SDHA disrupt CII integrity, alter CI stability, and ultimately compromise mitochondrial bioenergetic flexibility. This case further illustrates that SDHA-related disease in childhood can manifest with a milder, predominantly neurological phenotype characterized by epilepsy, global neurodevelopmental delay, and optic atrophy, contrasting with severe Leigh syndrome commonly associated with *SDHA* recessive inheritance. These findings emphasize the importance of functional studies to reclassify variants of uncertain significance and considering *SDHA* in the genetic workup of pediatric neurodevelopmental disorders with suspected mitochondrial involvement.

Funding source

This research was funded by the Instituto de Salud Carlos III, (ISCIII) and the Ministerio de Ciencia e Innovación (Madrid, Spain; co-funded by European Regional Development Fund "A way to make Europe"), grant number PI21/00381 to M.A.M. This work was also partially funded by the Agencia Estatal de Investigación, Grant Number PID2023-150506OB-I00.

CRediT authorship contribution statement

Rocío Garrido-Moraga: Writing – original draft, Visualization, Investigation, Formal analysis. **Pablo Serrano-Lorenzo:** Investigation, Formal analysis. **María J. Esteban-Amo:** Visualization, Validation. **Marcello Bellusci:** Resources, Formal analysis. **Miguel Á. de la Fuente:** . **Joaquín Arenas:** Resources, Formal analysis. **Adrián González-Quintana:** Resources, Formal analysis. **Cristina Ugalde:** Supervision, Methodology, Conceptualization. **María Simarro:** Writing – review & editing, Supervision, Funding acquisition. **Miguel A. Martín:** Writing – review & editing, Supervision, Funding acquisition, Conceptualization.

Declaration of competing interest

The authors declare that they have no known competing financial

interests or personal relationships that could have appeared to influence the work reported in this paper.

Acknowledgements

This research was funded by the Instituto de Salud Carlos III (ISCIII) and the Ministerio de Ciencia e Innovación (Madrid, Spain; co-funded by European Regional Development Fund "A way to make Europe"), grant number PI21/00381 to M.A.M. This work was also partially funded by the Agencia Estatal de Investigación, Grant Number PID2023-150506OB-I00. We sincerely acknowledge the generous participation of the patient's family in this study.

Appendix A. Supplementary data

Supplementary data to this article can be found online at https://doi.org/10.1016/j.mito.2026.102149.

References

Al Khazal, F.J., Bhat, S.M., Zhu, Y., de Araujo Correia, C.M., Zhou, S.X., Wilbanks, B.A., Folmes, C.D., Sieck, G.C., Favier, J., Maher, L.J., 2024. Similar deficiencies, different outcomes: succinate dehydrogenase loss in adrenal medulla vs. fibroblast cell culture models of paraganglioma. Cancer Metab. 12. https://doi.org/10.1186/s40170-024-00369-9.

Alston, C.L., Davison, J.E., Meloni, F., van der Westhuizen, F.H., He, L., Hornig-Do, H.T., Peet, A.C., Gissen, P., Goffrini, P., Ferrero, I., Wassmer, E., McFarland, R., Taylor, R. W., 2012. Recessive germline SDHA and SDHB mutations causing leukodystrophy and isolated mitochondrial complex II deficiency. J. Med. Genet. 49, 569–577. https://doi.org/10.1136/jmedgenet-2012-101146.

Anderson, S., Bankier, A.T., Barrell, B.G., De Bruijn, M.H.L., Coulson, A.R., Drouin, J., Eperon, I.C., Nierlich, D.P., Roe, B.A., Sanger, F., Schreier, P.H., Smith, A.J.H., Staden, R., Young, I.G., 1981. Sequence and organization of the human mitochondrial genome. Nature 290, 457–465. https://doi.org/10.1038/290457A0;KWRD=SCIENCE.

Bezawork-Geleta, A., Rohlena, J., Dong, L., Pacak, K., Neuzil, J., 2017. Mitochondrial complex II: At the Crossroads. Trends Biochem. Sci 42, 312–325. https://doi.org/10.1016/j.tibs.2017.01.003.

Bezawork-Geleta, A., Wen, H., Dong, L., Yan, B., Vider, J., Boukalova, S., Krobova, L., Vanova, K., Zobalova, R., Sobol, M., Hozak, P., Novais, S.M., Caisova, V., Abaffy, P., Naraine, R., Pang, Y., Zaw, T., Zhang, P., Sindelka, R., Kubista, M., Zuryn, S., Molloy, M.P., Berridge, M.V., Pacak, K., Rohlena, J., Park, S., Neuzil, J., 2018. Alternative assembly of respiratory complex II connects energy stress to metabolic checkpoints. Nat. Commun. 9. https://doi.org/10.1038/s41467-018-04603-z.

Boikos, S.A., Pappo, A.S., Killian, J.K., Laquaglia, M.P., Weldon, C.B., George, S., Trent, J. C., Von Mehren, M., Wright, J.A., Schiffman, J.D., Raygada, M., Pacak, K., Meltzer, P.S., Miettinen, M.M., Stratakis, C., Janeway, K.A., Helman, L.J., Author, J. O., 2016. Molecular Subtypes of KIT/PDGFRA Wild-Type Gastrointestinal Stromal Tumors: a Report from the National Institutes of Health Gastrointestinal Stromal Tumor Clinic HHS Public Access author manuscript. JAMA Oncol. 2, 922–928. https://doi.org/10.1001/jamaoncol.2016.0256.

Bujan, N., Morén, C., García-García, F.J., Blázquez, A., Carnicer, C., Cortés, A.B., González, C., López-Gallardo, E., Lozano, E., Moliner, S., Gort, L., Tobías, E., Delmiro, A., Martin, M.Á., Fernández-Moreno, M.Á., Ruiz-Pesini, E., Garcia-Arumí, E., Rodríguez-Aguilera, J.C., Garrabou, G., 2022. Multicentric standardization of protocols for the diagnosis of human mitochondrial respiratory chain Defects. Antioxidants 11, 741. https://doi.org/10.3390/ANTIOX11040741/S1.

Cao, K., Xu, J., Cao, W., Wang, X., Lv, W., Zeng, M., Zou, X., Liu, J., Feng, Z., 2023. Assembly of mitochondrial succinate dehydrogenase in human health and disease. Free Radic. Biol. Med. 207, 247–259. https://doi.org/10.1016/J.FREERADBIOMED.2023.07.023.

Cardaci, S., Zheng, L., Mackay, G., Van Den Broek, N.J.F., Mackenzie, E.D., Nixon, C., Stevenson, D., Tumanov, S., Bulusu, V., Kamphorst, J.J., Vazquez, A., Fleming, S., Schiavi, F., Kalna, G., Blyth, K., Strathdee, D., Gottlieb, E., 2015. Pyruvate carboxylation enables growth of SDH-deficient cells by supporting aspartate biosynthesis. Nat. Cell Biol. 17. https://doi.org/10.1038/ncb3233.

Chen, C.L., Ishihara, T., Pal, S., Huang, W.L., Ogasawara, E., Chang, C.R., Ishihara, N., 2024. SDHAF2 facilitates mitochondrial respiration through stabilizing succinate dehydrogenase and cytochrome c oxidase assemblies. Mitochondrion 79, 101952. https://doi.org/10.1016/J.MITO.2024.101952.

Darin, N., Oldfors, A., Moslemi, A.R., Holme, E., Tulinius, M., 2001. The incidence of mitochondrial encephalomyopathies in childhood: Clinical features and morphological, biochemical, and DNA abnormalities. Ann. Neurol. 49, 377–383. https://doi.org/10.1002/ANA.75.

Dhingra, V., Kirshenbaum, L.A., 2015. Succinate dehydrogenase/complex II activity obligatorily links mitochondrial reserve respiratory capacity to cell survival in cardiac myocytes. Cell Death Dis. 6, e1956–e. https://doi.org/10.1038/CDDIS.2015.310;TECHMETA.

Du, Z., Zhou, X., Lai, Y., Xu, J., Zhang, Y., Zhou, S., Feng, Z., Yu, L., Tang, Y., Wang, W., Yu, Lu., Tian, C., Ran, T., Chen, H., Guddat, L.W., Liu, F., Gao, Y., Rao, Z., Gong, H., 2023. Structure of the human respiratory complex II. Proc. Natl. Acad. Sci. 120, e2216713120. https://doi.org/10.1073/PNAS.2216713120.

Dwight, T., Benn, D.E., Clarkson, A., Vilain, R., Lipton, L., Robinson, B.G., Clifton-Bligh, R.J., Gill, A.J., 2013. Loss of SDHA expression identifies SDHA mutations in succinate dehydrogenase-deficient gastrointestinal stromal tumors. Am. J. Surg. Pathol. 37, 226–233. https://doi.org/10.1097/PAS.0B013E3182671155.

Fernández-Vizarra, E., Ferrín, G., Pérez-Martos, A., Fernández-Silva, P., Zeviani, M., Enríquez, J.A., 2010. Isolation of mitochondria for biogenetical studies: an update. Mitochondrion 10, 253–262. https://doi.org/10.1016/j.mito.2009.12.148.

Fullerton, M., McFarland, R., Taylor, R.W., Alston, C.L., 2020. The genetic basis of isolated mitochondrial complex II deficiency. Mol. Genet. Metab. 131, 53–65. https://doi.org/10.1016/J.YMGME.2020.09.009.

Gault, M.D., Mandelker, D., Delair, D., Stewart, C.R., Kemel, Y., Sheehan, M.R., Siegel, B., Kennedy, J., Marcell, V., Arnold, A., Al-Ahmadie, H., Modak, S., Robson, M., Shukla, N., Roberts, S., Vijai, J., Topka, S., Kentsis, A., Cadoo, K., Carlo, M., Schwark, A.L., Reznik, E., Dinatale, R., Hechtman, J., Flores, E.B., Jairam, S., Yang, C., Li, Y., Can Bayraktar, E., Ceyhan-Birsoy, O., Zhang, L., Kohlman, W., Schiffman, J., Stadler, Z., Birsoy, K., Kung, A., Offit, K., Walsh, M.F., 2018. Germline SDHA Mutations in Children and Adults with Cancer. https://doi.org/10.1101/mcs.a002584.

González-Quintana, A., García-Consuegra, I., Belanger-Quintana, A., Serrano-Lorenzo, P., Lucia, A., Blázquez, A., Docampo, J., Ugalde, C., Morán, M., Arenas, J., Martín, M. A., 2020. Novel NDUFA13 Mutations Associated with OXPHOS Deficiency and Leigh Syndrome: A Second Family Report. Genes 2020, Vol. 11, Page 855 11, 855. Doi: 10.3390/GENES11080855.

Greggio, C., Jha, P., Kulkarni, S.S., Lagarrigue, S., Broskey, N.T., Boutant, M., Wang, X., Conde Alonso, S., Ofori, E., Auwerx, J., Cantó, C., Amati, F., 2017. Enhanced respiratory chain supercomplex formation in response to exercise in human skeletal muscle. Cell Metab. 25, 301–311. https://doi.org/10.1016/J.CMET.2016.11.004.

H Sturrock, B.R., Macnamara, E.F., McGuire, P., Kruk, S., Yang, I., Murphy, J., Diseases Network, U., Tifft, C.J., Gordon-Lipkin, E., Ellen Macnamara, C.F., 2021. Progressive cerebellar atrophy in a patient with complex II and III deficiency and a novel deleterious variant in SDHA: A Counseling Conundrum. Mol Genet Genomic Med 9, 1692. Doi: 10.1002/mgg3.1692.

Hart, M.L., Quon, E., Vigil, A.-L.-B., Engstrom, I.A., Newsom, O.J., Davidsen, K., Hoellerbauer, P., Carlisle, S.M., Sullivan, L.B., 2023. Mitochondrial redox adaptations enable alternative aspartate synthesis in SDH-deficient cells. Elife 12. https://doi.org/10.7554/elife.78654.

Ikeda, K., Shiba, S., Horie-Inoue, K., Shimokata, K., Inoue, S., 2013. A stabilizing factor for mitochondrial respiratory supercomplex assembly regulates energy metabolism in muscle. Nat. Commun. 4, 1–9. https://doi.org/10.1038/NCOMMS3147;SUBJMETA.

Iverson, T.M., Singh, P.K., Cecchini, G., 2023. An evolving view of complex II-noncanonical complexes, megacomplexes, respiration, signaling, and beyond. J. Biol. Chem. 299, 104761. https://doi.org/10.1016/j.jbc.2023.104761.

Koopman, W.J.H., Willems, P.H.G.M., Smeitink, J.A.M., 2012. Mechanisms of Disease Monogenic Mitochondrial Disorders. N. Engl. J. Med.

Korpershoek, E., Favier, J., Gaal, J., Burnichon, N., Van Gessel, B., Oudijk, L., Badoual, C., Gadessaud, N., Venisse, A., Bayley, J.P., Van Dooren, M.F., De Herder, W.W., Tissier, F., Plouin, P.F., Van Nederveen, F.H., Dinjens, W.N.M., Gimenez-Roqueplo, A.P., De Krijger, R.R., 2011. SDHA immunohistochemistry detects germline SDHA gene mutations in apparently sporadic paragangliomas and pheochromocytomas. J. Clin. Endocrinol. Metab. 96, E1472–E1476. https://doi.org/10.1210/JC.2011-1043.

Lorendeau, D., Rinaldi, G., Boon, R., Spincemaille, P., Metzger, K., Jäger, C., Christen, S., Dong, X., Kuenen, S., Voordeckers, K., Verstreken, P., Cassiman, D., Vermeersch, P., Verfaillie, C., Hiller, K., Fendt, S.M., 2017. Dual loss of succinate dehydrogenase (SDH) and complex I activity is necessary to recapitulate the metabolic phenotype of SDH mutant tumors. Metab. Eng. 43, 187–197. https://doi.org/10.1016/J.YMBEN.2016.11.005.

Morán, M., Rivera, H., Sánchez-Aragó, Blázquez, A., Merinero, B., Ugalde, C., Arenas, J., Cuezva, J.M., Martín, M.A., 2010. Mitochondrial bioenergetics and dynamics interplay in complex I-deficient fibroblasts. Biochimica et Biophysica Acta (BBA) - Molecular Basis of Disease 1802, 443–453. Doi: 10.1016/J.BBADIS.2010.02.001.

Ng, Y.S., Turnbull, D.M., 2016. Mitochondrial disease: genetics and management. J. Neurol. 263, 179–191. https://doi.org/10.1007/S00415-015-7884-3.

Pettersen, E.F., Goddard, T.D., Huang, C.C., Meng, E.C., Couch, G.S., Croll, T.I., Morris, J. H., Ferrin, T.E., 2021. UCSF ChimeraX: Structure visualization for researchers, educators, and developers. Protein Sci. 30, 70–82. https://doi.org/10.1002/pro.3943.

Pfanner, N., Warscheid, B., Wiedemann, N., 2019. Mitochondrial proteins: from biogenesis to functional networks. Nat. Rev. Mol. Cell Biol. https://doi.org/10.1038/s41580-018-0092-0.

Renkema, G.H., Wortmann, S.B., Smeets, R.J., Venselaar, H., Antoine, M., Visser, G., Ben-Omran, T., van den Heuvel, L.P., Timmers, H.J.L.M., Smeitink, J.A., Rodenburg, R.J. T., 2015. SDHA mutations causing a multisystem mitochondrial disease: novel mutations and genetic overlap with hereditary tumors. European Journal of Human Genetics 2015 23:2 23, 202–209. Doi: 10.1038/ejhg.2014.80.

Richards, S., Aziz, N., Bale, S., Bick, D., Das, S., Gastier-Foster, J., Grody, W.W., Hegde, M., Lyon, E., Spector, E., Voelkerding, K., Rehm, H.L., 2015. Standards and guidelines for the interpretation of sequence variants: a joint consensus recommendation of the American College of Medical Genetics and Genomics and the Association for Molecular Pathology. Genet. Med. 17, 405–424. https://doi.org/10.1038/gim.2015.30.

Rutter, J., Winge, D.R., Schiffman, J.D., 2010. Succinate dehydrogenase - Assembly, regulation and role in human disease. Mitochondrion 10, 393–401. https://doi.org/10.1016/j.mito.2010.03.001.

Sievers, F., Wilm, A., Dineen, D., Gibson, T.J., Karplus, K., Li, W., Lopez, R., McWilliam, H., Remmert, M., Söding, J., Thompson, J.D., Higgins, D.G., 2011. Fast, scalable generation of high-quality protein multiple sequence alignments using Clustal Omega. Mol. Syst. Biol. 7. https://doi.org/10.1038/msb.2011.75.

Timón-Gómez, A., Pérez-Pérez, R., Nyvltova, E., Ugalde, C., Fontanesi, F., Barrientos, A., 2020. Protocol for the Analysis of yeast and Human Mitochondrial respiratory Chain Complexes and Supercomplexes by Blue Native Electrophoresis. STAR Protoc. 1. https://doi.org/10.1016/J.XPRO.2020.100089.

van de Loo, K.F.E., Custers, J.A.E., de Boer, L., van Lieshout, M., de Vries, M.C., Janssen, M.C.H., Verhaak, C.M., 2022. Cognitive functioning and mental health in children with a primary mitochondrial disease. Orphanet J. Rare Dis. 17, 1–13. https://doi.org/10.1186/S13023-022-02510-7/TABLES/3.

Wang, K., Li, M., Hakonarson, H., 2010. ANNOVAR: Functional annotation of genetic variants from high-throughput sequencing data. Nucleic Acids Res. 38. https://doi.org/10.1093/nar/gkq603.

Waterhouse, A., Bertoni, M., Bienert, S., Studer, G., Tauriello, G., Gumienny, R., Heer, F. T., De Beer, T.A.P., Rempfer, C., Bordoli, L., Lepore, R., Schwede, T., 2018. SWISS-MODEL: homology modelling of protein structures and complexes. Nucleic Acids Res. 46. https://doi.org/10.1093/nar/gky427.